X-ray Diffraction Tomographic Imaging and Reconstruction

Ke Chen and David Castañón
ECE Department, Boston University {ck, dac}@bu.edu

Abstract

Material discrimination based on conventional or dual energy X-ray computed tomography (CT) imaging can be ambiguous. X-ray diffraction imaging (XDI) can be used to construct diffraction profiles of objects, providing new molecular signature information that can be used to characterize the presence of specific materials. Combining X-ray CT and diffraction imaging can lead to enhanced detection and identification of explosives in luggage screening. In this work we are investigating techniques for joint reconstruction of CT absorption and X-ray diffraction profile images of objects to achieve improved image quality and enhanced material classification. The initial results have been validated via simulation of X-ray absorption and coherent scattering in 2 dimensions.

Background

X-ray Diffraction Imaging

- X-ray scattering types: coherent and incoherent
- XDI makes use of coherently scattered X-ray to reconstruct the coherent-scatter form factor
- XDI identifies material based on their molecular composition
- **Form factor** $|F(q)|^2$
  - expressed in transferred momentum q that causes the deviation of photon of wavelength λ by angle θ : $q = \lambda^{-1}\sin(\theta/2)$
  - reveal Bragg peaks for material discrimination

XDI State-of-the-Art[1]

Morpho XRD 3500™

- Direct imaging rather than tomographic
- Probe with polychromatic X-ray radiation
- Measure coherent scattering with energy-resolving detectors
- Require line collimators to localize scattering location under investigation
- Often used as confirmation sensor for ambiguous regions in CT
- Can be slow

Methodologies

XDI Imaging Modality

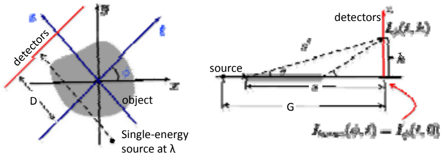

Schematic drawing of XDT system: left x-y plane, right y-z plane.

$$I_\phi(t,h)=\int_0^G I_o(t,0)A(t,s,0)B(t,s,h)|F(t,s,h)|^2\mathcal{E}(t,s,h)ds$$

$$I_{trans}(\phi,t)=\int_0^G I_o(t,0)A(t,s,0)B(t,s,0)\mathcal{E}_{CT}ds$$

$I_o(t,0)$: incident x-ray intensity;
$A(t,s,0)$: attenuation along the incoming ray;
$B(t,s,h)$: attenuation along the scattered ray;
$|F(t,s,h)|^2$: form factor at $q=\lambda^{-1}\sin(\arctan(h/s)/2)$;

$$\left.\begin{aligned}\mathcal{E}(t,s,h)&=\frac{G-s}{(h^2+(G-s)^2)^{3/2}}\\ \mathcal{E}_{CT}&=1/G^2\end{aligned}\right\}$$ geometrical efficiency factor.

Filtered Backprojection (FBP) reconstruction[2]

Assumption:

- Collimator blades are used to restrict measurements to scattering perpendicular to excitation plane
- Attenuation along the path of scattered radiation is independent of the scattering angle $B(t,s,h)=B(t,s,0)$

Measurement:

$$P_\phi(t,h)=\frac{I_\phi(t,h)}{I_{trans}(\phi,t)}=\int_0^G|F(t,s,h)|^2\xi(t,s,h)ds$$

where $\xi(t,s,h)=\dfrac{G^2(G-s)}{(h^2+(G-s)^2)^{3/2}}$

Algorithm:

$$|F(x,y,q)|^2=\int_\phi\int_t\int_h\xi^{-1}(t,s,h)Q_\phi(t,h)\delta(\bar{t}-t)\delta(\frac{h}{2\lambda s}-q)dhdtd\phi$$

Where $Q_\phi(t,h)=\int_{-\infty}^{+\infty}P_\phi(t',h)g(t-t')dt'$, $g(\cdot)$ is a ramp filter

$$s=D+x\sin\phi-y\cos\phi$$
$$\bar{t}=x\cos\phi+y\sin\phi$$

Algebraic reconstruction[3]

$$y=Ax$$

where y of size m is a stack of intensity measurements, x is a stack of q-images to be estimated, and A denotes the forward operator.

Algorithm: for the *k*-th iteration, updates with the relaxation parameter ρ_k as following

$$x^{k,0}=x^k$$
$$x^{k,i}=x^{k,i-1}+\rho_k\frac{y_i-\langle a^i,x^{k,i-1}\rangle}{\|a^i\|_2^2},\quad i=1,\dots,m$$
$$x^{k+1}=x^{k,m}$$

where a^i denotes the *i*-th row of A.

Experiment and Results

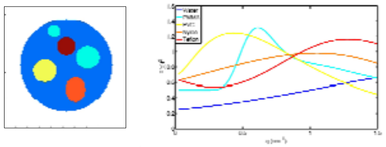

Phantom and synthetic diffraction profile priors

A phantom with size 105×105 mm consisting of 5 materials and air as background was centered at the origin. A mono-energetic X-ray parallel beam of 60KeV was used to probe the phantom. Given form factor priors, diffraction patterns were simulated on a detector of size 100(height)×151(width) mm placed 620 mm away from the origin. 90 projections were collected for reconstruction.

Filtered backprojection reconstructions were generated for different levels of additive noise under various Gaussian noise. Every pixel in the reconstructed fields was assigned to the class that minimizes the Euclidean distance from the reconstructed diffraction profile to the priors.

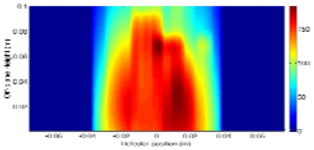

Simulated diffraction patterns at 45° viewing angle.

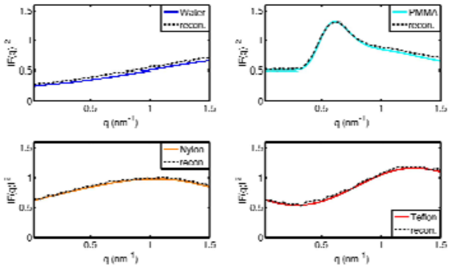

FBP reconstruction of diffraction profile at SNR=20dB.

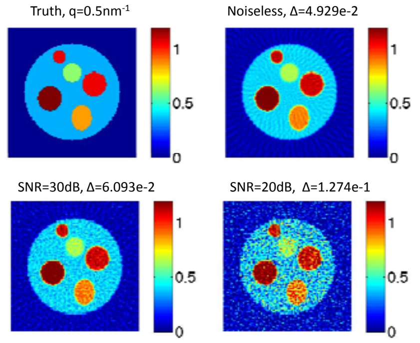

Truth, $q=0.5nm^{-1}$ — Noiseless, Δ=4.929e-2

SNR=30dB, Δ=6.093e-2 — SNR=20dB, Δ=1.274e-1

FBP Reconstruction at $q=0.5nm^{-1}$ at various noise level.

Discussion

The initial results are encouraging, but are limited by the fidelity of the simulation model, which is similar to the model used in the reconstruction algorithm. We are exploring integration of higher fidelity X-ray models based on Monte Carlo techniques. We also want to explore algorithms that avoid the independence assumption of the scattering paths, requiring algebraic inversion, and perform joint reconstruction and recognition.

The resulting algorithms can lead to new generations of X-ray diffraction imaging sensors that have higher photon counts than current systems by capturing additional scattering directions. The approach can be combined with multi-energy illumination and photon counting detectors, as well as advanced inversion techniques.

Future Work

- Develop fast algebraic reconstruction algorithm
- Apply robust joint multi-frequency inversion. techniques developed in [4] to XDT for improved reconstruction and recognition.
- Extend the work for polychromatic X-ray radiation with limited-angles.

References

[1] G. Harding and et al., "Radiation source considerations relevant to next-generation x-ray diffraction imaging for security screening applications", Proc. SPIE, Vol. 7450, 2009.
[2] U. Stevandaal and et al., "A reconstruction algorithm for coherent scatter computed tomography based on filtered back-projection", *Med. Phys.*, 30(9), pp. 2465—2474, 2003.
[3] S. Schneider and et al., "Coherent Scatter Computed Tomography Applying a Fan-Beam Geometry", Proc. SPIE, Vol. 4320, pp. 754—763, 2001.
[4] K. Chen, D. Castañón, "Robust Multifrequency Inversion in Terahertz Diffraction Tomography", to appear in SPIE Defense, Security, and Sensing, April 2011.

This material is based upon work supported by the U.S. Department of Homeland Security under Award Number 2008-ST-061-ED0001. The views and conclusions contained in this document are those of the authors and should not be interpreted as necessarily representing the official policies, either expressed or implied of the U.S. Department of Homeland Security.